Phase-locked Local Oscillator for Superconducting Integrated Receiver

Valery P. Koshelets[1,2,*], Andrey B. Ermakov[1,2], Pavel N. Dmitriev[1], Lyudmila V. Filippenko[1], Andrey V. Khudchenko[1,2], Nickolay V. Kinev[1,2], Oleg S. Kiselev[1,2], Irina L. Lapitskaya[1], Alexander S. Sobolev[1,2], and Mikhail Yu. Torgashin[1,2]

[1]*Institute of Radio Engineering and Electronics (IREE), Russia*

[2]*SRON Netherlands Institute for Space Research, Groningen, the Netherlands*

* Contact: valery@hitech.cplire.ru, phone +7-495-629 3418

***Abstract*— A Superconducting Integrated Receiver (SIR) comprises in a single chip a planar antenna combined with a superconductor-insulator-superconductor (SIS) mixer, a superconducting Flux Flow Oscillator (FFO) acting as a Local Oscillator (LO) and a second SIS harmonic mixer (HM) for the FFO phase locking. In this report an overview of the FFO development and optimization is presented. In order to overcome temperature constraints and extend operation frequency of the fully Nb SIR we have developed and studied Nb-AlN-NbN circuits with a gap voltage Vg up to 3.7 mV and extremely low leak currents (Rj/Rn > 30). Continuous tuning of the frequency due to bending and overlapping of the Fiske steps and a possibility to phase lock the Nb-AlN-NbN FFO at any frequency in the range 350-750 GHz has been experimentally demonstrated. After optimization of the FFO design the free-running linewidth between 7 and 1.5 MHz has been measured in the frequency range 350 – 750 GHz, which allows to phase-lock from 50 to 95 % of the emitted FFO power. New designs of the FFO intended for further improvement of its parameters are under development, but even at the present state the Nb-AlN-NbN FFOs are mature enough for practical applications. These achievements enabled development of a 500 - 650 GHz integrated receiver for the Terahertz Limb Sounder (TELIS) project intended for atmosphere study and scheduled to fly on a balloon in 2008.**

I. Introduction

A Superconducting Integrated Receiver (SIR) [1], [2] was proposed more than 10 years ago and finally has been developed for practical applications [3], [4]. A SIR comprises in one chip (size of 4 mm*4 mm*0.5 mm) a low-noise SIS mixer with quasioptical antenna, an FFO [5] acting as a Local Oscillator (LO) and a second SIS harmonic mixer (HM) for the FFO phase locking, see Fig. 1. The concept of the SIR looks very attractive for many practical applications due to SIR compactness and a wide tuning range of the FFO [6]. Presently, the frequency range of the most practical heterodyne receivers is limited by the tunability of the local oscillator. For a solid-state multiplier chain the fractional input bandwidth typically does not exceed 10-15 %. In the SIR the bandwidth is determined by the SIS mixer tuning structure and matching circuitry between the SIS and the FFO; bandwidth up to 30 - 40 % may be achieved with a twin-junction SIS mixer design.

Free-running linewidth of the FFO can be up to 10 MHz; so to obtain the frequency resolution required for practical application of a heterodyne spectrometer (of at least one part per million) the integrated local oscillator (LO) must be stabilized. To achieve this goal a concept of the integrated receiver with the FFO phase-locked to an external reference has been developed [7], [8]. To prove capability of the SIR for high-resolution spectroscopy we have successfully measured line profiles of OCS gas around 625 GHz [3]. Latest results on development of a 500 - 650 GHz integrated receiver for the Terahertz Limb Sounder (TELIS) project [9], [10] are presented at this Symposium [11].

There is a number of important requirements on the FFO properties to make it suitable for application in the phase- locked SIR. Obviously the FFO should emit enough power to pump an SIS mixer (taking into account a specially designed mismatch of about 5-7 dB between the FFO and the SIS mixer, introduced to avoid leakage of the input signal to the LO path). It is a challenge to realize the ultimate performance of separate superconducting elements after their integration in a single-chip device. Implementation of the improved matching circuits and submicron junctions for both the SIS and the HM allows delivering optimal FFO power for their operation.

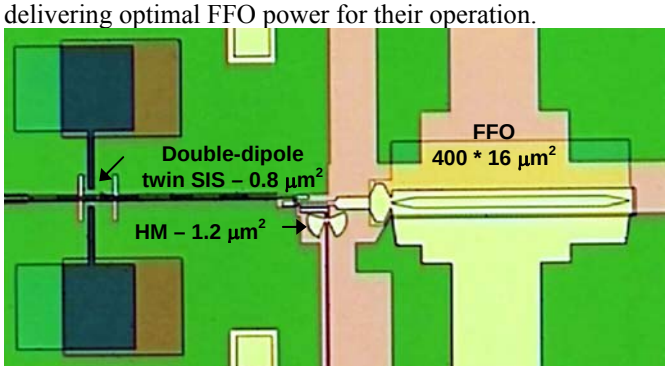

Fig. 1. Central part of the SIR chip with double-dipole antenna, twin SIS-mixer and harmonic mixer for FFO phase locking.

Even for ultra wideband room-temperature PLL system an effective regulation bandwidth is limited by length of the cables in the loop (about 10 MHz for typical loop length of two meters). It means that free-running FFO linewidth has to be well below 10 MHz to ensure stable FFO phase locking with reasonably good spectral ratio (SR) - the ratio between the carrier and total power emitted by the FFO [6]. For example, only about 50 % of the FFO power can be phase-locked by the present PLL system at free-running FFO linewidth of 5 MHz. Low spectral ratio results in considerable error at resolving of the complicated line shape [8]. Thus sufficiently small free-running FFO linewidth is vitally important for realization of the phase-locked SIR for the TELIS.

Earlier the Nb-AlOx-Nb or Nb-AlN-Nb trilayers were successfully used for the SIR fabrication. Traditional all-Nb circuits are being constantly optimized but there seems to be a limit for linewidth optimizations at certain boundary frequencies due to Josephson self-coupling (JSC) effect [12] as well as a high frequency limit, imposed by Nb gap frequency (~700 GHz). That is the reason for novel types of junctions based on materials other than Nb to be developed.

We reported on development of the high quality Nb-AlN-NbN junction production technology [13]. The implementation of an AlN tunnel barrier in combination with an NbN top superconducting electrode provides a significant improvement in SIS junction quality. The gap voltage of the junction Vg = 3.7 mV. From this value, the gap voltage of the Nb film Δ_{Nb}/e = 1.4 mV and the voltage of the singularity corresponding to the difference of the superconducting gaps of the junction contacts $V_\delta = (\Delta_{NbN} - \Delta_{Nb})/e$ = 0.9 mV we estimated the gap voltage of our NbN film as Δ_{NbN}/e = 2.3 mV [14].

The dependency of the ratio of subgap to normal state resistance (Rj/Rn) vs. critical current density (Jc) for different types of the Nb based junctions fabricated at IREE is presented in Fig. 2. One can see that the Nb-AlN-NbN junctions have very good quality at high current densities that is important for implementation in THz mixers. The same technique was further used to produce complicated integrated circuits comprising SIS and FFO in one chip.

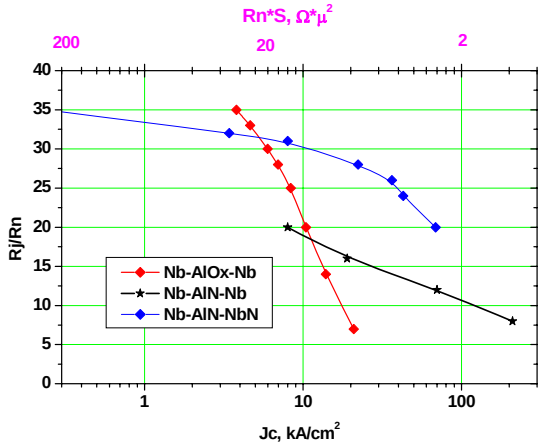

Fig. 2. The dependencies of Rj/Rn ratio vs. critical current density Jc for junctions fabricated at IREE [14].

II. Nb-AlN-NbN Flux Flow Oscillator

A Josephson Flux Flow Oscillator (FFO) [5] has proven to be the most developed superconducting local oscillator for integration with an SIS mixer in a single-chip submm-wave Superconducting Integrated Receiver [1] - [4]. The FFO is a long Josephson tunnel junction of the overlap geometry (see Fig. 3) in which an applied dc magnetic field and a dc bias current, I_B, drive a unidirectional flow of fluxons, each containing one magnetic flux quantum, $\Phi_0 = h/2e \approx 2*10^{-15}$ Wb. Symbol h is Planck's constant and e is the elementary charge. An integrated control line with current I_{CL} is used to generate the dc magnetic field applied to the FFO. According to the Josephson relation the junction oscillates with a frequency $f = (1/\Phi_0)*V$ (about 483.6 GHz/mV) if it is biased at voltage V. The fluxons repel each other and form a chain that moves along the junction. The velocity and density of the fluxon chain and thus the power and frequency of the mm-wave signal emitted from the exit end of the junction due to the collision with the boundary may be adjusted independently by I_B and I_{CL}. The FFO differs from the other members of the Josephson oscillator family by the need for these two control currents, which in turn provides the possibility of independent frequency and power tuning.

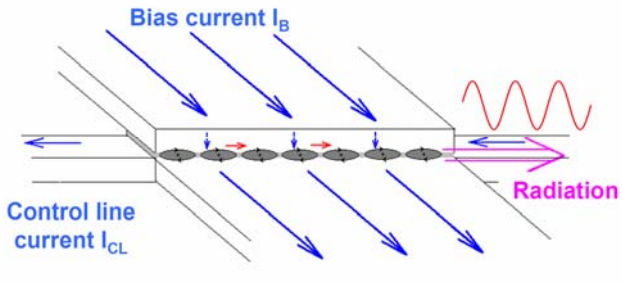

Fig. 3. Schematic view of the Flux-Flow Oscillator.

The length, L, and the width, W, of the FFO used in this study are 300 - 400 μm and 4 - 28 μm,, respectively. The value of the critical current density, Jc, is in the range 4 - 8 kA/cm^2 giving a Josephson penetration depth, $\lambda_J \sim$ 6 - 4 μm. The corresponding value of the specific resistance is $Rn*L*W$ *is* ~ 50 - 25 Ohm*μm^2. For the numerical calculations we use a typical value of the London penetration depth, $\lambda_L \approx$ 90 nm, and a junction specific capacitance, $Cs \approx$ 0.08 pF/ μm^2. The active area of the FFO (i. e. the AlO_x or the AlN tunnel barrier) is usually formed as a long window in the relatively thick (200-250 nm) SiO_2 insulation layer sandwiched between the

two superconducting films (base and wiring electrodes). The so-called "idle" region consisting of the thick SiO_2 layer adjacent to the junction (on both sides of the tunnel region) between the overlapping electrodes forms a transmission line parallel to the FFO. The width of the idle region (W_I = 2 - 14 μm) is comparable to the junction width. The idle region must be taken into account when designing an FFO with desired properties. In our design it is practical to use the flat bottom electrode of the FFO as a control line in which the current I_{CL} produces the magnetic field, which mainly is applied perpendicular to the long side of the junction (see Fig. 3).

The use of Nb for top "wiring" layer is preferable due to lower losses of Nb compared to NbN below 720 GHz; furthermore, the matching structures developed for the all-Nb SIRs can be used directly for the fabrication of receivers with Nb-AlN-NbN junctions. General behaviour of the new devices is similar to the all-Nb ones; even the control currents, necessary to provide magnetic bias for FFO, were nearly the same for the FFOs of similar design.

A family of the Nb-AlN-NbN FFO IVCs measured at different magnetic fields produced by the integrated control line is presented in Fig. 4 (L= 300 μm, W = 14 μm, W_I= 10 μm). Single SIS junction with inductive tuning circuit is employed as a HM for the linewidth measurements. The tuning and matching circuits were designed to provide "uniform" coupling in the frequency range 400 –700 GHz. Measured value of the HM current induced by the FFO oscillations (HM pumping) is shown in Fig. 4 by the color scale. The HM pumping for each FFO bias point was measured at constant HM bias voltage 3 mV (pumping is normalized on the current jump at the gap voltage, I_g = 140 μA). From Fig. 4 one can see that an

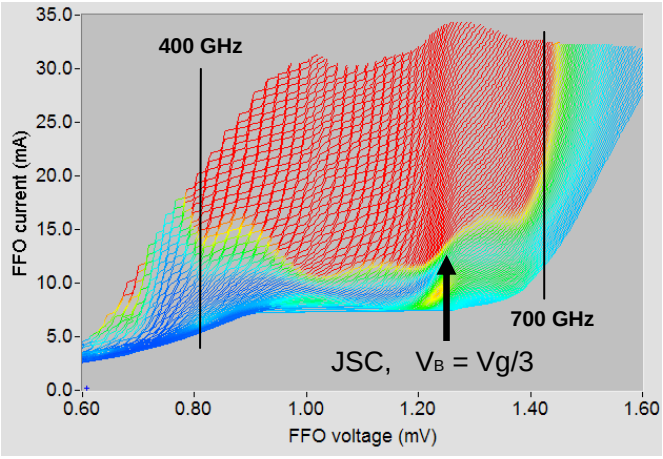

Fig. 4. (Color online) IVCs of the Nb-AlN-NbN-Nb FFO measured at different magnetic fields produced by the integrated control line. The color scale shows the level of the DC current rise at the HM induced by the FFO. Red area marks the region of the FFO parameters where the induced by FFO HM current exceeds 25% of the Ig. This level is well above the optimal value for an SIS-mixer operation.

FFO can provide large enough power over the wide frequency range limited at higher frequencies only by Nb superconducting gap in transmission line electrodes (base and wiring layers) and by design of the matching circuits below 400 GHz. The Nb-AlN-NbN FFOs behave very similar to all-Nb ones. The feature at about 600 GHz where the curves get denser is a JSC (Josephson Self-Coupling) boundary voltage was firstly observed for all-Nb FFOs [12]. The JSC effect (absorption of the emitted by an FFO *ac* radiation by the quasi-particles in the cavity of the long junction) considerably modifies FFO properties at the voltages $V \approx V_{JSC} = 1/3*Vg$ (V_{JSC} corresponds to 620 GHz for the Nb-AlN-NbN FFO). Just above this voltage differential resistance increases considerably; that results in FFO linewidth broadening just above this point. This, in turn, makes difficult or impossible phase-locking of the FFO in that region. For Nb-AlOx-Nb FFO a transition, corresponding *to* $V_{JSC} = Vg/3$ occurs around 450 GHz. So, we can cover the frequency gap from 450 to 550 GHz imposed by the gap value of all-Nb junctions using the Nb-AlN-NbN FFOs. Feature on the graph (around 500 GHz) is very likely due to singularity at difference of the superconducting gaps $\Delta_{NbN} - \Delta_{Nb}$.

Continuous frequency tuning at frequencies below 600 GHz for the Nb-AlN-NbN FFOs of moderate length becomes possible though the damping is not high enough to completely suppress Fiske resonant structure at frequencies below Vg/3. For short junctions with small α – wave attenuation factor, the distance between the steps in this resonant regime can be as large, that it is only possible to tune the FFO at the certain set of frequencies. For 300-400 μm long Nb-AlN-NbN junction this is not the case – the quality factor of the resonator formed by a long Nb-AlN-NbN-Nb Josephson junction is not so high at frequencies > 350 GHz; the resonance steps are slanting and the distance between them is not so big (see Fig. 4). That allows us to set any voltage (and any frequency) below V_{JSC}, but for each voltage only a certain set of currents should be used. So, in this case we have the regions of forbidden bias current values, specific for each voltage below V_{JSC}, instead of the forbidden voltage regions for Fiske regime in Nb-AlOx-Nb FFO [14]. Special algorithms have been developed for automatic working point selection in flight; details are presented in [15].

In Fig. 5 typical current-voltage characteristics (IVCs) of a Nb-AlN-NbN SIS junction (area ~ 1.5 μm^2), pumped by a Nb-AlN-NbN FFO (solid line – unpumped IVC, dotted lines – pumped by the FFO at different frequencies). One can see that the FFO provides more than enough power for the mixer pumping (in this experiment we use the test circuits with low-loss matching circuits tuned between 400 and 700 GHz). Even at the specially introduced 5 dB FFO/SIS mismatch (required for the SIR operation) the FFO delivers enough power for the SIS mixer operation in complete TELIS range 490-650 GHz [6].

An important issue for the SIR operation is a possibility to tune the FFO power keeping constant FFO frequency. This is demonstrated in Fig. 6, where the IVCs of an SIS mixer, pumped at different FFO bias currents (different powers) are shown. Dependence of the SIS pump current on the FFO bias current is presented in Fig. 7. One can see that FFO power can be tuned in the range more than 15 dB keeping the same frequency by proper adjustment of the control line current.

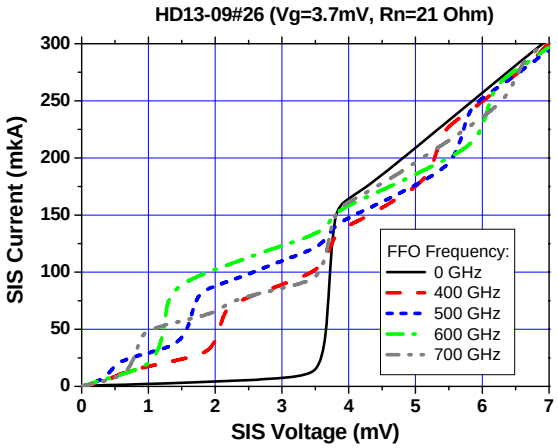

Fig. 5. The IVCs of the SIS mixer.; unpumped – solid curve, pumped at different frequencies – dashed and dotted lines [14].

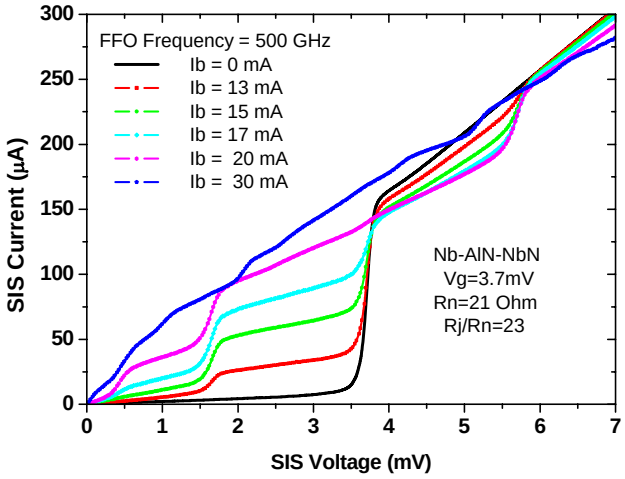

Fig. 6. The IVCs of the SIS mixer; unpumped – black solid curve, pumped at different FFO bias currents (different powers) – lines with symbols.

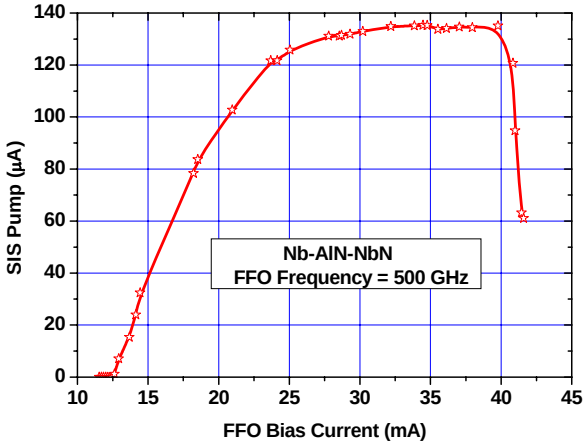

Fig. 7. The pump current of the SIS mixer biased at 3 mV as a function of the FFO bias current (see Fig. 4 and 6).

III. Spectral Properties of an FFO

A. Linewidth Measurements

The FFO linewidth (LW) has been measured in a wide frequency range from 300 GHz up to 750 GHz using a well-developed experimental technique [16]. We investigated the linewidth of the Nb-AlN-NbN FFOs by the same setup, as was used for linewidth measurement of the all-Nb FFO. A specially designed integrated circuit incorporates the FFO junction, the SIS harmonic mixer and the microwave matching circuits. Generally, both junctions are fabricated from the same Nb/AlN/NbN or Nb/AlOx/Nb trilayer. The FFO signal is fed to the SIS harmonic mixer (HM) together with a 17 – 20 GHz reference signal from a stable synthesizer. The required power level depends on the parameters of the HM; it is about of 1 μW for a typical junction area of 1 μm^2. The intermediate frequency (IF) mixer product ($f_{IF} = \pm (f_{FFO} - n \cdot f_{SYN})$ at ~ *400 MHz* is first boosted by a cooled HEMT amplifier (T_n ~ 5 K, gain = 30 dB) and then by a high-gain room temperature amplifier. The resulting IF signal is supplied to the Phase-Locking loop (PLL) system for FFO stabilization (frequency or phase lock). The phase-difference signal of the PLL is fed to the FFO control line current. Wideband operation of the PLL (10-15 MHz full width) is obtained by minimizing the cable loop length. A part of the IF signal is delivered to the spectrum analyzer via a power splitter. All instruments are synchronized to harmonics of a common 10 MHz reference oscillator.

The integrated harmonic mixer may operate in two different regimes, either as quasi-particle mixer (SIS) or as Josephson mixer. In order to exclude the noise from the Josephson super-current fluctuations and thereby realize a pure quasi-particle regime the super current has to be suppressed by a relatively large magnetic field. This requires a special control line placed near the SIS mixer.

Quasi-particle regime of the HM operation could be realised also at high enough level of the synthesizer power. It has been shown [17] that the FFO linewidth and signal-to-noise ratio are almost the same for these two regimes, although the phase noise is somewhat lower in the quasi-particle mode.

In order to accurately measure the FFO line shape the IF signal must be time-averaged by the spectrum analyzer. To remove low frequency drift and interference from the bias supplies, temperature drift, etc. we use a narrow bandwidth (< 10 kHz) Frequency Discriminator (FD) system with relatively low loop gain for *frequency locking* of the FFO. With the FD narrow-band feedback system that stabilizes the mean frequency of the FFO we can accurately measure the free-running FFO linewidth, which is determined by the much faster internal ('natural") fluctuations.

Most measurement procedures can be controlled by a computer-based data acquisition (DAQ) system that have automatic routines for many standard tests and can perform user-programmed specialized measurements [15].

B. Dependence of the FFO Linewidth on FFO' Parameters

Detailed measurements of the FFO linewidth [18], [19] demonstrate Lorentzian shape of the FFO line in a wide frequency range up to 750 GHz, both at higher voltages on the flux flow step (FFS) and at lower voltages in the resonant regime on the Fiske steps (FS's). It means that the free-running ("natural") FFO linewidth in all operational regimes is determined by the wideband thermal fluctuations and the shot noise (the same as for Nb-AlOx-Nb junctions). This is different from many traditional microwave oscillators where the "natural" linewidth is very small and the observed linewidth can be attributed mainly to external fluctuations. It was found [18], [19] that free-running FFO linewidth, δf, exceed theoretical estimations made for lumped tunnel Josephson junction. The expression for LW dependency on voltage and differential resistances found for all-Nb FFOs [18], [20] is valid for Nb-AlN-NbN junctions as well:

$$\delta f = (2\pi/\Phi_0^2)\,(R_d^B + K^*R_d^{CL})^2\, S_i(0); \qquad (1)$$

where $S_i(0)$ is the power density of low frequency current fluctuations, R_d^B and R_d^{CL} are differential resistances on bias and control line currents respectively. Note that ratio R_d^{CL}/R_d^B is constant for fixed FFO bias, so $\delta f = A(I_B)\,(R_d^B)^2\, S_i(0)$.

Earlier so-called Super Fine Resonance Structure (SFRS) [21] was observed on the FFO IVCs; this structure results in the jumps of the FFO between tiny steps (frequency spacing is of about 10 MHz, see Fig. 8). Presence of the SFRS makes impossible phase locking at frequencies between steps that is unacceptable for practical applications. Recently we found that the SFRS is related to interference of the acoustic waves created by the FFO (generation of the phonons by Josephson junction is well possible [22]). Special technological procedure allows us to eliminate this interference and realize continuous FFO frequency tuning in the SIR that was vitally important for TELIS project (see Fig. 8). Details of this study will be published elsewhere.

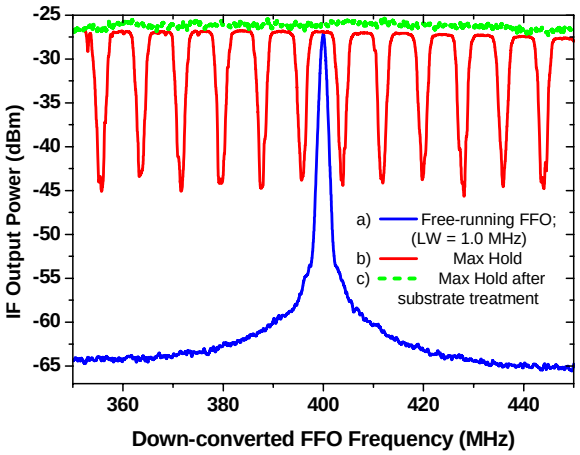

Fig. 8. Down-converted spectra of the FFO: a) Free-running FFO; b), c) - Signal recorded in the MaxHold regime of the Spectrum Analyzer at fine tuning of the FFO frequency recorded before and after special Si substrate treatment.

In Fig. 9 we present comparative graph of the FFO linewidth for two types of the tri-layer. One can see that the linewidth of Nb-AlN-NbN-Nb FFO is twice as small up to 600 GHz. It should be emphasized that due to FS overlapping continuous tuning is possible and any desirable frequency could be realized. Several "stacked" stars at certain frequencies for the NbN FFO mean that the best linewidth value can be selected by adjusting FFO bias (all the linewidth values at the selected frequency are close and any will actually be good for measurements). Each star corresponds to an "allowed" bias current at Fiske steps (as described above in section II). Although the FFO tuning on FS is complicated, the benefit in linewidth (and, consequently, spectral ratio) is worth the trouble – LW below 3 MHz can be achieved in the whole range between 350 – 610 GHz. Abrupt increase of the FFO linewidth at some frequencies is caused by Josephson self-coupling effect. The JSC (absorption of the emitted by an FFO ac radiation by the quasi-particles in the cavity of the long junction, see above) considerably modifies FFO properties at the voltages $V \approx V_{JSC} = 1/3^*V_g$ [12] (V_{JSC} corresponds to 620 GHz for the Nb-AlN-NbN FFO).

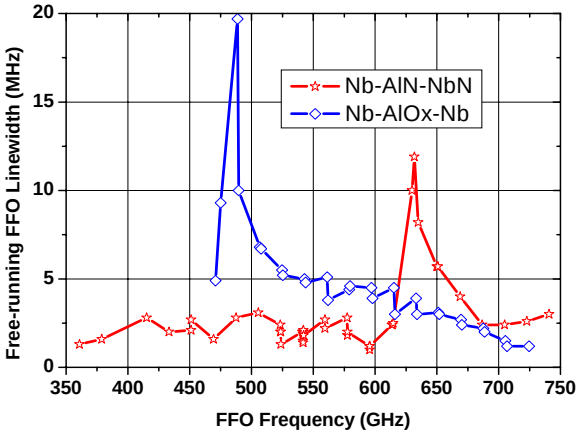

Fig. 9. Linewidth dependency on frequency for two types of the FFO [14].

Employment of NbN electrode does not result in noise increase and the linewidth as low as 0.5 MHz was measured at 600 GHz. It allows us to phase lock up to 97 % of the emitted FFO power and realize very low phase noise about – 90 dBc (see below). Our observations made for junctions of different topology let us assume that all dependencies of the linewidth on the junction parameters known for all-Nb FFOs hold for the Nb-AlN-NbN ones. For example, we observe that the linewidth decreases with junction width increase.

Previous linewidth measurements have demonstrated [6], [23] essential dependence of the free-running FFO linewidth on the FFO voltage, its current density and geometry of the biasing electrodes. In this report we summarized results of the FFO study and optimization of the FFO layout for both types of the FFO. Recently it was shown [4], [6] that the linewidth decreases considerably with increasing FFO width, *W,* of the junction. This is valid for all frequencies of interest, and consequently the Spectral Ratio of the phase locked FFO for wide junctions is higher. We have increased the FFO width up to 28 μm, which is more than five times the Josephson penetration depth λ_J. A number of FFOs with the same electrode layout, but different width of the FFO junction (W = 4, 8, 12, 16, 20 and 28 μm) are fabricated using the same technological procedure yielding the same junction parameters (normal state resistance * area, RnS = 30 Ω*μm^2). The results of the linewidth measurements of these circuits at three frequencies are presented in Fig. 10.

Even for the largest tested width (W = 28 μm) there is no evidence of deterioration in the FFO behaviour. Furthermore, power delivered to the SIS mixer is getting higher and the linewidth lower at all frequencies. The decrease of the FFO linewidth with increasing FFO width is in accordance with existing theoretical models and our expectations. The bias current differential resistance, *Rd,* decreases approximately inversely proportional to the bias current I_B. Since the FFO linewidth is proportional to Rd^2*I_B, it scales down linearly with the junction width. Of course, one can expect that the linewidth decrease will saturate and the FFO performance will deteriorate with further increase of the width (e.g., due to appearance of transversal modes). Due to lack of a reliable theory the optimal value of the FFO width has to be determined experimentally. Note that for a wider FFO the centre line of the junction is shifted away from the edge of the control line (the R_d^{CL} goes down). This may result in a considerable reduction of extraneous noise from external magnetic fields. Furthermore, a wider FFO presumably will have a more uniform bias current distribution [4]. At the present state width of the FFO for TELIS project is chosen to be 16 μm – trade-off between linewidth requirements and technical limitation on maximum bias and control line currents (both should not exceed 70 mA).

In contrast with variation of the FFO linewidth on the FFO width previous measurements [6] have demonstrated a considerable increase of the FFO linewidth with the FFO current density. It contradicts the simplified consideration: the increase of the FFO current density (as it is for increase of the FFO width) should result in the increase of the total FFO bias current, I_B, and reduce the FFO differential resistance on the bias current R_d. Since the FFO linewidth is proportional to $R_d^2*I_b$ one should expect the decrease of the measured FFO free-running linewidth for larger FFO current density. In reality R_d does not decrease as much as this simple consideration predicts and the linewidth increases. From the other hand high value of the current density ($J_c \geq 8$ kA/cm^2) is important for wide-band operation of the SIS-mixer at the submm wave range. The discussed above increase of the FFO linewidth with current density creates serious problem in design and development of SIR chips. Implementation of two separate tri-layers with different current densities - one for the SIS mixer (high J_c) and the other one for the FFO/HM (lower J_c) might be a solution. We have successfully tested and verified this approach for SIR TELIS microcircuits.

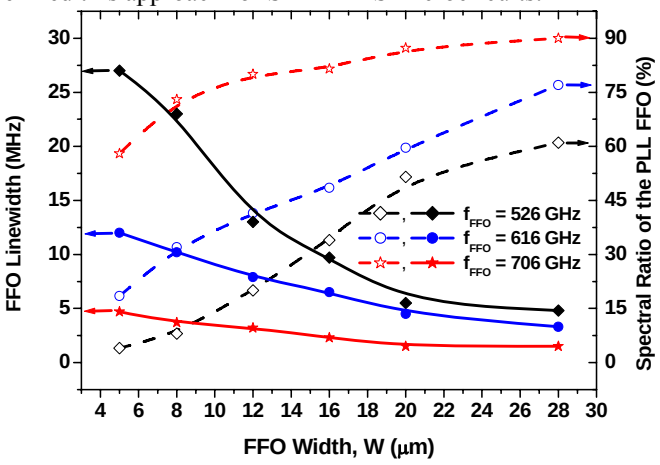

Fig. 10. Linewidth of free-running FFOs (left axis) and corresponding Spectral Ratio for the phase-locked FFO (right axis) measured at different FFO frequencies as a function of FFO width. All circuits are

fabricated using the same technological procedure (RnS = 30 Ω*μm^2) [4].

Improvement of the performance was obtained for the FFO with enlarged electrodes overlapping. Larger overlapping presumably provides more uniform bias current distribution – due to much smaller inductance of the overlapping electrodes. Larger overlapping of the FFO electrodes means also that the FFO of the same width is shifted from the edge of the bottom electrode that results in considerable decrease of the R_d^{CL} value. Note that for wide FFO some shift of the FFO centerline appears "automatically" due to increasing of the width. Experimentally we found that idle region W_I = 10 μm is optimal value for present FFO design. Up to now there is no adequate model that can describe quantitatively both the processes in the FFO and a self-consistent distribution of the bias current. Nevertheless, presented results are very encouraging and these modifications of the FFO were implemented in the TELIS SIRs.

To explore further this approach we developed different designs of the "self-shielded" FFO with large ground plane. Such FFO supposed to be much more protected from variations of external magnetic field and has to provide more uniform bias current distribution (since all bias leads are laying over superconducting shield and have low inductance). Actually, low inductive bias leads provide a possibility of optimal (rather than uniform) current distribution, "requested" by the FFO itself. The last feature must ensure maximum of emitted FFO power. Indeed, the IVCs of all shielded FFOs are much more reproducible; the power, delivered to HM is higher compared to a "standard" design. Unfortunately, free-running linewidth for all variants of shielded FFO with separate bias leads is much larger than linewidth for FFO of traditional design. It seems that injection of the bias via separate leads results in some spatial modulation of bias current [23] despite the additional triangular elements added for more uniform current injection. From other hand, designs that employed three superconducting electrodes provide both perfect pumping and improved linewidth, details will be published elsewhere.

C. Spectral Ratio, Phase Noise

As it was mentioned above free-running FFO linewidth has to be well below 10 MHz to ensure stable FFO phase locking with reasonably good spectral ratio (SR) - the ratio between the carrier and total power emitted by FFO. For example, only about 50 % of the FFO power can be phase-locked by the present TELIS PLL system at free-running FFO linewidth of 5 MHz. Low spectral ratio results in considerable error at resolving of the complicated line shape [8]. The SR value for the given PLL system is determined by free-running FFO linewidth: these two quantities are unambiguously related (see Fig. 11 where data for FFO of different designs and types are presented). Theoretical curve, calculated in [24], coincides reasonably with experimental data. A possibility to increase considerably the SR by application of the ultra-wideband cryogenic PLL system has been recently demonstrated [25].

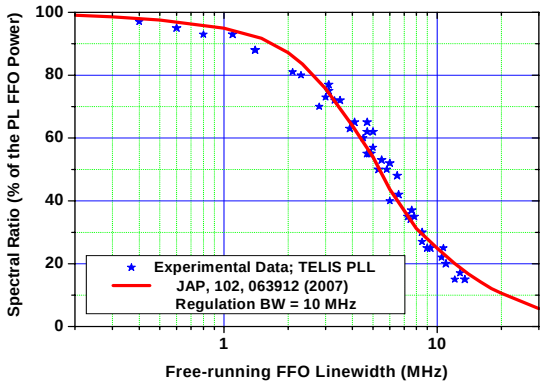

Fig. 11. Spectral Ratio for the phase-locked FFO of different types and designs as a function of free-running FFO linewidth. Solid line – calculated dependence of the SR on FFO LW for PLL bandwidth = 10 MHz [24].

An important issue for TELIS operation is a possibility to tune the FFO frequency and power independently providing the same spectral ratio of PL FFO. The TELIS HM is pumped by a tunable reference frequency in the range of 19-21 GHz from the Local oscillator Source Unit (LSU), phase locked to the internal ultra stable 10 MHz Master Oscillator. The HM mixes the FFO signal with the n-th harmonic of the 19-21 GHz reference. Linewidth and SR for the FFO of TELIS design are almost constant over very wide range of FFO bias current at fixed FFO frequency (see Fig. 12). From this figure one can see that the SR is of about 50 % over the range of bias current, I_b, 14 – 30 mA, while the pumping level varies from 3.5 μA at I_b = 14 mA up to 81 μA at I_b = 30 mA. Furthermore, the SR = 34% can be realized at I_b = 12 mA where the HM pumping is below 0.5 μA. It means that the HM operates in highly non-linear regime and even moderate HM pumping is enough for efficient PLL operation ensuring large enough signal to noise ratio.

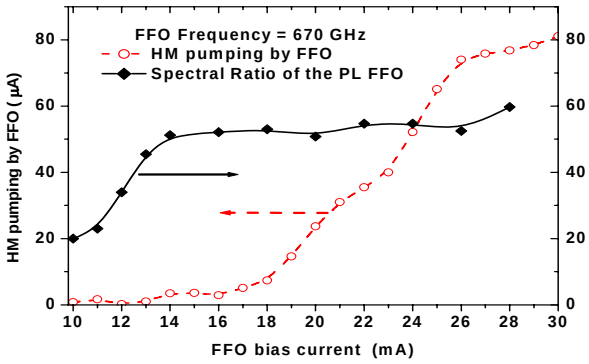

Fig. 12. Dependence of the HM current induced by FFO (HM pumping) and Spectral Ratio after FFO phase locking as a function of FFO bias current. All data measured at FFO frequency of 670 GHz [6].

After optimization of the FFO design the free-running linewidth between 7 and 0.5 MHz has been measured in the frequency range 350 – 750 GHz (see Fig. 10), which allows to phase-lock from 35 to 95 % of the emitted FFO. Example of the free-running (frequency-locked) and phase-locked spectra of the FFO measured for flight SIR at one of the frequencies selected for first TELIS flight are presented in Fig. 13. Data for five important TELIS frequencies are summarized in Table 1. It should be mentioned that noise of the digital electronics at frequencies of about 1 MHz slightly increases measured linewidth value; while the PLL is able to suppress the interference that results in large SR than can be expected from measured linewidth. Note also dependence of the SR and LW on the FFO bias current related to variation of the differential resistance along Fiske step.

To investigate frequency resolution of the receiver we have measured the signal of the synthesizer multiplied by a super-lattice structure [26]. The signal recorded in these measurements is a convolution of the delta-function provided by synthesizer with phase-locked spectra of the FFO with accuracy of the used resolution bandwidth of the spectrum analyzer (30 kHz), so the frequency resolution of the receiver is not worse than 100 kHz.

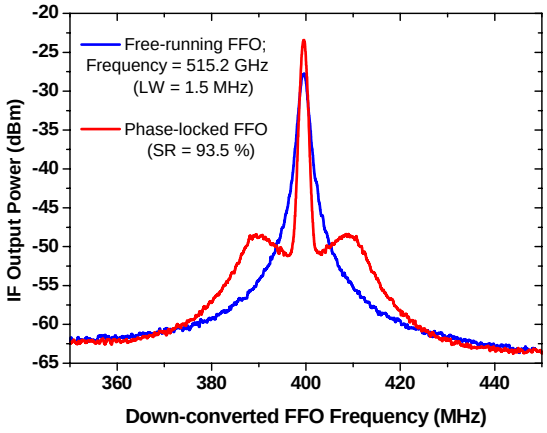

Fig. 13. Spectra of the FFO operating at 515.2 GHz (red curve – frequency locked; blue curve – phase-locked). Linewidth (LW) = 1.5 MHz; Signal to Noise Ratio (SNR) = 36 dB; Spectral Ration (SR) = 93.5 %. Spectra measured with RBW = 1 MHz, span = 100 MHz.

TABLE VI
DATA FOR THE FLIGHT SIR AT SELECTED TELIS FREQUENCIES

FFO Frequency (GHz)	LW (MHz)	SNR (dB)	SR (%)	FFO Ib (mA)
495.0	1.5	32	90	30.7
496.9	1.5	37	93	31.3
515.2	1.5	36	93.5	29.2
607.7	2.1	32	87.7	30
607.7	1.8	32.6	88.6	34
619.1	5.4	25	63.3	30
619.1	4.6	26.8	70.3	34

To prove capability of the SIR for high-resolution spectroscopy line profiles of OCS gas around 625 GHz have been successfully measured by the SIR operating in the DSB regime [3]. The tests were done in a laboratory gas cell setup at a gas pressure down to 0.2 mBar, corresponding to the FWHM linewidth <5 MHz. It was demonstrated that spectrum recorded by the Digital Auto Correlator (DAC) is a convolution product of the signal (gas emission lines) with the FFO line spectrum; resolution in this experiment is limited by DAC back-end.

The residual phase noise of the phase locked FFO - measured relative to the reference synthesizer - is plotted in Fig. 4 as function of the offset from the carrier. To get absolute FFO phase noise, one should add the synthesizer noise multiplied by n^2 to the residual phase noise of the FFO. Data for the R&S®SMF100A Microwave Signal Generator with improved phase noise [27] are also presented in Fig. 14. For the case where the FFO, operating at 450 GHz, is locked to the 20-th harmonic of the synthesizer, $n^2 = 400$. The total (absolute) FFO phase noise (solid line in Fig. 14) is dominated by the synthesizer noise for offsets < 10 kHz. The noise at larger frequency offset is mainly due to PLL system. Note that the FFO phase noise is overestimated since no subtraction of the noise added by the IF amplifier chain was performed; actually at offsets much larger than the PLL regulation bandwidth (> 20 MHz) measured phase noise is mainly determined by the IF chain.

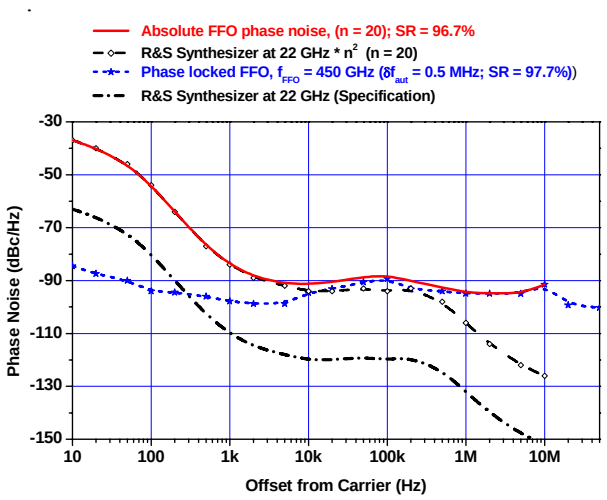

Fig. 14. Experimental phase noise of a phase locked FFO at 450 GHz. Since the phase noise of the FFO is measured relative to the 20th harmonic of the synthesizer, the synthesizer noise [27], multiplied by a factor $20^2 = 400$, should be added to the residual FFO noise to get the total (absolute) FFO phase noise – solid red line.

CONCLUSIONS

In conclusion, optimized design of the FFO for TELIS has been developed and tested. Free-running linewidth value from 7 to 0.5 MHz has been measured in the frequency range 300 – 750 GHz for "wide" FFO. As a result the spectral ratio of the phased-locked FFO varies from 35 to 95 % correspondingly, ensure at least of half phase-locked FFO power in the frequency range 300-750 GHz. The "unlocked" rest of the total FFO power increases the phase noise and the calibration error

Continuous tuning of the frequency is possible for Nb-AlN-NbN FFO due to bending and overlapping of the Fiske steps, so that any desirable frequency can be realized. A possibility to phase lock the Nb-AlN-NbN FFO at any frequency in the range 350-750 GHz has been experimentally demonstrated. New designs of the FFO intended for further improvement of its parameters are under development, but even at the present state the Nb-AlN-NbN FFOs are mature enough for practical applications.

Phase–locked SIR operation over frequency range 450 – 700 GHz has been realized, spectral resolution below 1 MHz has been confirmed by CW signal measurements. An uncorrected double side band (DSB) noise temperature below 150 K has been measured for the SIR with the phase-locked FFO and the intermediate frequency bandwidth 4 - 8 GHz. To ensure remote operation of the phase-locked SIR several procedures for its automatic computer control have been developed and tested.

ACKNOWLEDGMENT

Authors thank Pavel Yagoubov, Gert de Lange and Wolfgang Wild for fruitful and stimulating discussions, as well as Vladimir Vaks, Oleksandr Pylypenko and Dimitry Paveliev for development of the dedicated components for TELIS.

The work was supported in parts by the RFBR projects 06-02-17206, the ISTC project # 3174, NATO SfP Grant 981415, and the Grant for the Leading Scientific School 5408.2008.2

REFERENCES

[1] V.P. Koshelets, S.V. Shitov, L.V. Filippenko, A.M. Baryshev, H. Golstein, T. de Graauw, W. Luinge, H. Schaeffer, H. van de Stadt "First Implementation of a Superconducting Integrated Receiver at 450 GHz"; *Appl. Phys. Lett.*, vol. 68, No. 9, pp. 1273-1275, Feb 1996.

[2] V. P. Koshelets and S. V. Shitov, "Integrated Superconducting Receivers," *Superconductor Science and Technology*, vol. 13, pp. R53-R69, 2000.

[3] P. Yagoubov, R. Hoogeveen, M. Torgashin, A. Khudchenko, V. Koshelets, N. Suttiwong, G. Wagner, M. Birk, "550-650 GHz spectrometer development for TELIS", *The 17th International Symposium on Space Terahertz Technology*, Paris, May 2006, Conference Proceedings ISSTT 2006, report FR3-3, pp. 338-341.

[4] V.P. Koshelets, A.B. Ermakov, L.V. Filippenko, A.V. Khudchenko, O.S. Kiselev, A.S. Sobolev, M.Yu. Torgashin, P.A. Yagoubov, R.W.M. Hoogeveen, and W. Wild, "Iintegrated Submillimeter Receiver for TELIS", "*IEEE Trans. on Appl. Supercond.",* vol. 17, pp 336-342, 2007.

[5] T. Nagatsuma, K. Enpuku, F. Irie, and K. Yoshida, "Flux-flow type Josephson oscillator for millimeter and submillimeter wave region," *J. Appl. Phys.,* vol. 54**,** p. 3302, 1983, see also Pt. II: *J. Appl. Phys.* Vol. 56**,** p. 3284, 1984; Pt. III, *J. Appl. Phys., vol.* 58**,** p. 441, 1985; Pt. IV, *J. Appl. Phys.*, vol. 63, p. 1130, 1988.

[6] V.P. Koshelets, P.N. Dmitriev, A.B. Ermakov, A.S. Sobolev, M.Yu. Torgashin, V.V. Kurin, A.L. Pankratov, J. Mygind, "Optimization of the Phase-Locked Flux-Flow Oscillator for the Submm Integrated Receiver", "*IEEE Trans. on Appl. Supercond.",* vol. 15, pp. 964-967, 2005.

[7] V.P. Koshelets, S.V. Shitov, A.V. Shchukin, L.V. Filippenko, P.N. Dmitriev, V.L. Vaks, J. Mygind, A.B. Baryshev, W. Luinge, H. Golstein, "Flux Flow Oscillators for Sub-mm Wave Integrated Receivers", *IEEE Trans. on Appl. Supercond.,* **v.9,** No 2, pp. 4133-4136, 1999.

[8] V.P. Koshelets, S.V. Shitov, A.B. Ermakov, O.V. Koryukin, L.V. Filippenko, A. V. Khudchenko, M. Yu. Torgashin,P. Yagoubov, R. Hoogeveen, O.M. Pylypenko, "Superconducting Integrated Receiver for TELIS", "*IEEE Trans. on Appl. Supercond.",* vol. 15, pp. 960-963, 2005.

[9] R.W.M. Hoogeveen, P.A. Yagoubov, A. de Lange, A.M. Selig, V.P. Koshelets, B.N. Ellison and M. Birk, "Superconducting Integrated Receiver development for TELIS", presented at the 12th International Symposium on Remote Sensing, 19-22 September 2005, Bruges, Belgium. Sensors, Systems, and Next-Generation Satellites IX; Roland Meynart, Steven P. Neeck, Haruhisa Shimoda; Eds., Proc. of SPIE, vol. 5978 (2005), p. 440-450.

[10] R.W.M. Hoogeveen, P.A. Yagoubov, G. de Lange, A. de Lange, V. Koshelets, M. Birk, B. Ellison, "Balloon borne heterodyne stratospheric limb sounder TELIS ready for flight", presented at the SPIE European Remote Sensing Conference 2007 in Florence, September 2007; SPIE European Remote Sensing Conference, Proceedings of SPIE, 6744, 67441U-1- 67441U-10, 2007.

[11] Gert de Lange, Pavel Yagoubov, Hans Golstein, Leo de Jong, Arno de Lange, Bart van Kuik, Ed de Vries, Johannes Dercksen, Ruud Hoogeveen, Valery Koshelets, Andrey Ermakov, and Lyudmila Filippenko, "Flight configuration of the TELIS instrument", presented at the *19th International Symposium on Space Terahertz Technology*

[12] *(ISSTT-08)*, Groningen, the Netherlands, April 2008, report 10-2; this Proceedings.

[13] V. P. Koshelets, S. V. Shitov, A. V. Shchukin, L. V. Filippenko, J. Mygind, and A. V. Ustinov, "Self-Pumping Effects and Radiation Linewidth of Josephson Flux Flow Oscillators", *Phys Rev B*, vol. 56, p. 5572-5577, 1997.

[14] P.N. Dmitriev, I.L. Lapitskaya, L.V. Filippenko, A.B. Ermakov, S.V. Shitov, G.V. Prokopenko, S.A. Kovtonyuk, and V.P. Koshelets. "High Quality Nb-based Integrated Circuits for High Frequency and Digital Applications", "*IEEE Trans. on Appl. Supercond.",* vol. 13, No 2, pp. 107-110, June 2003.

[15] M.Yu. Torgashin, V.P. Koshelets, P.N. Dmitriev, A.B. Ermakov, L.V.Filippenko, and P.A. Yagoubov, "Superconducting Integrated Receivers based on Nb-AlN-NbN circuits" presented at the Applied Superconductivity Conference ASC-2006. Seattle, USA, August 2006, report 3EG08, "*IEEE Trans. on Appl. Supercond.",* vol. 17, pp.379- 382, 2007.

[16] A.B. Ermakov, O.S. Kiselev, V.P. Koshelets, P.A. Yagoubov, G. de Lange, B. van Kuik, "Superconducting Integrated Receiver for TELIS optimization and computer control", presented at the *19th International Symposium on Space Terahertz Technology (ISSTT-08)*, Groningen, the Netherlands, April 2008, report P6-5.

[17] V.P. Koshelets, S.V. Shitov, A.V. Shchukin, L.V. Filippenko, and J. Mygind, "Linewidth of Submillimeter Wave Flux-Flow Oscillators"; *Appl. Phys. Lett.*, vol. **69,** pp. 699-701, July 1996.

[18] V.P. Koshelets and J. Mygind, **"**Flux Flow Oscillators For Superconducting Integrated Submm Wave Receivers", Studies of High Temperature Superconductors, edited by A.V. Narlikar, NOVA Science Publishers, New York, vol. 39, pp. 213-244, 2001.

[19] V.P. Koshelets, A.B. Ermakov, P.N. Dmitriev, A.S. Sobolev, A.M. Baryshev, P.R. Wesselius, J. Mygind, "Radiation linewidth of flux flow oscillators", *Superconductor Science and Technology,* **v. 14,** pp. 1040 - 1043, 2001.

[20] V.P. Koshelets, S.V. Shitov, P.N. Dmitriev, A.B. Ermakov, L.V. Filippenko, V.V. Khodos, V.L. Vaks, A.M. Baryshev, P.R. Wesselius, J. Mygind, "Towards a Phase-Locked Superconducting Integrated Receiver: Prospects and Limitations", *Physica C*, **367,** pp. 249 - 255, 2002.

[21] A. L. Pankratov, "Form and width of spectral line of a Josephson flux flow oscillator", *Phys. Rev. B*, vol. 65, p. 054504-(1-9), 2002.

[22] V.P. Koshelets, A.B. Ermakov, S.V. Shitov, P.N. Dmitriev, L.V. Filippenko, A.M. Baryshev, W. Luinge, J. Mygind, V.L. Vaks, D.G. Pavel'ev, "Superfine Resonant Structure on IVC of Long Josephson Junctions and its Influence on Flux Flow Oscillator Linewidth", *IEEE Trans. on Appl. Supercond.,* **v.11,** No 1, pp. 1211-1214, 2001.

[23] P. Berberich, R. Buemann, and H. Kinder, "Monochromatic Phonon Generation be the Josephson Effect", Phys. Rev. Lett, vol. 49, No. 20, pp. 1500 – 1503, Nov. 1982.

[24] V.P. Koshelets, S.V. Shitov, L.V.Filippenko, P.N. Dmitriev, A.B. Ermakov, A.S. Sobolev, M.Yu. Torgashin, A.L. Pankratov, V.V. Kurin, P. Yagoubov, R. Hoogeveen. "Superconducting Phase-Locked Local Oscillator for a Submm Integrated Receiver", *Superconducting Science and Technology*, **v.** 17, pp. $127-$131, 2004.

[25] A.L. Pankratov, V.L. Vaks, and V.P. Koshelets, "Spectral properties of phase locked Flux Flow Oscillator", *Journal of Applied Physics,* vol. 102, 0629, pp. 1-5, 2007.

[26] A.V. Khudchenko, V.P. Koshelets, P.N. Dmitriev, A.B. Ermakov, P.A. Yagoubov, and O.M. Pylypenko, "Cryogenic Phase Detector for Superconducting Integrated Receiver" "*IEEE Trans. on Appl. Supercond.",* vol. 17, pp. 606-608, 2007.

[27] E. Schomburg, R. Scheuerer, S. Brandl, K.F. Renk, D.G. Paveliev, Yu. Koschurinov, V. Ustinov, A. Zhukov, A. Kovsh, P.S. Kop`ev, *Electronics Letters,* vol.35, No.17, 1999.

[28] Specification of the R&S®SMF100A Microwave Signal Generator; Available: http://www2.rohde-schwarz.com/product/smf100a.html